Chimney and diverging effects in core PWR: analysis and experimental characterization for predictive behavior during loss of coolant accident

Christophe Rabe, Raphaël Préa

CHIMNEY AND DIVERGING EFFECTS IN CORE PWR: ANALYSIS AND EXPERIMENTAL CHARACTERIZATION FOR PREDICTIVE BEHAVIOR DURING LOSS OF COOLANT ACCIDENT

Christophe Rabe and Raphaël Préa
CEA – Commissariat à l'Energie Atomique et aux Energies Alternatives
DEN/DM2S/STMF – Service de Thermohydraulique et de Mécanique des Fluides
Université Paris-Saclay, F-91191, Gif-sur-Yvette, France
christophe.rabe@cea.fr ; raphael.prea@cea.fr

ABSTRACT

Safety analysis for Pressurized Water Reactors (PWR) currently uses systems code like CATHARE. In order to enhance the simulation of accidental transients studied, such as Large Break Loss of Coolant Accident (LBLOCA), 3D models have recently been developed. Although 3D modules for pressurized vessels were initially considered very coarse, CPU cost large decrease impulse a global refinement of the meshes used. In this way, if 3D nodalizations were only able at the beginning to describe large phenomena like radial power profile in the core or water liquid mass evolution in the downcomer during the refill phase, meshes that are used today could give accurate pieces of information on local scale like influence of spacer grids or flows between the subchannels during the reflood of the core. According to these new 3D modelisations, a better description of the chimney effect that could occur during the reflood phase of a LOCA accident could be given. Indeed, because of radial power difference between the assemblies in the core, liquid density, velocity and associated pressure in subchannels tend to modify the cross-flow and thus the axial flow that ensure rods cooling.
A physical description of the chimney and diverging phenomena is first given, before analysing their occurrences on experimental tests ran on PERICLES and ROSA-2/LSTF facilities. At last, a simulation of the influence of these phenomena for a dedicated modelisation of the reflood phase during a LOCA accident in PWR is proposed.

KEYWORDS

CHIMNEY EFFECT, LOCA, 3D, CATHARE, PWR

1. INTRODUCTION

System thermalhydraulics codes like CATHARE [1] have 3D modules in porous medium approach which were initially devoted to the prediction of very large scale 3D effects during LBLOCA. They were validated on the data of the 2D-3D experimental program performed in UPTF, SCTF or LOFT facilities (see [2] [3] [4] for the CATHARE validation against these facilities). 3D modules were used first with rather coarse reactor nodalization including only a few hundreds of meshes in the whole pressure vessel. Today the increased computer power allows 3D simulations with a much finer nodalization for many transients. A 3D vessel modelling with one mesh per assembly in the core is now available with the CATHARE code [5].
As 3D modules of system code are actually used for safety studies [6] and will be used for real-time simulators [7], their capabilities are analyzed [8] and 3D effects predicted by the 3D modules became a safety issues.
This article will focus on 3D effects occurring in the dry zone of the core during LOCA. In fact, as shown in this article, 3D effects have a direct impact on the Peak Cladding Temperature (PCT) of the rods. First,

part 2 gives an analysis of 3D cross-flow in PWR core. Then, experimental effects of cross flow are shown in part 3. At last, part 4 presents CATHARE calculations that point out the impact of these 3D effect on the PCT.

2. ANALYSIS OF THE 3D CROSS-FLOWS IN PWR CORE

D. Bestion has already analyzed the 3D core Thermalhydraulics phenomena in PWR LOCA [9], [10], [11]. In this part, we will first describe the global phenomenology occurring in the core during a LOCA transient, introducing the "Chimney" and "Diverging" effect in the dry zone. Then, we will revisit the F_1 number proposed by Bestion to characterize the "Chimney" and "Diverging" effect [9]. Axial acceleration will be considered too (it was not in the first Bestion analyze). Then, we will identify the main parameters influencing the F_1 number. To conclude, "Chimney" and "Diverging" effect at sub-channel scale will be described.

2.1. Global Phenomenology

During LOCA transients, core uncovering phases are expected. Due to a lack of water cooling, there may be a two phase mixture up to the swell level and a pure vapor flow in the upper part of the core. Such configuration takes place after the SCRAM when the power decay is below the 5% nominal power (5%NP). Under the swell level, water is generally at the saturation temperature and boiling occurs due to power decay. Hot assemblies with high power regions produce more vapor than the other ones and gravity driven natural circulation creates a radial flow from high power regions to low power regions. This phenomenon tends to homogenize the void fraction. Due to this radial homogenization, swell level is almost uniform. This has been experimentally observed [13] [15]. Indeed, the vapor mass flux leaving the swell level tends also to be homogenized according to radial flows.
In the dry zone, where cladding temperature excursion occurs the vapor flow is mainly axial. Higher cladding temperature could be observed in the highest power assembly. Then according to the radial power profile, cross-flow can occur between assemblies. Two situation could be observed: the "Chimney" effect, where cross-flow come from the lowest power assemblies to the higher power ones and "Diverging" effect, where cross-flows come from the highest power assemblies to the lower power ones. The cladding temperature is linked to the local vapor mass flux: higher cladding temperature are expected with lower mass flux. Thus cross-flows have an impact on the PCT: "Chimney" effect tends to decrease the PCT and "Diverging" effect conduct to an increase of the PCT by providing or removing cooling to the highest power assemblies. Fig. 1 presents both situations.

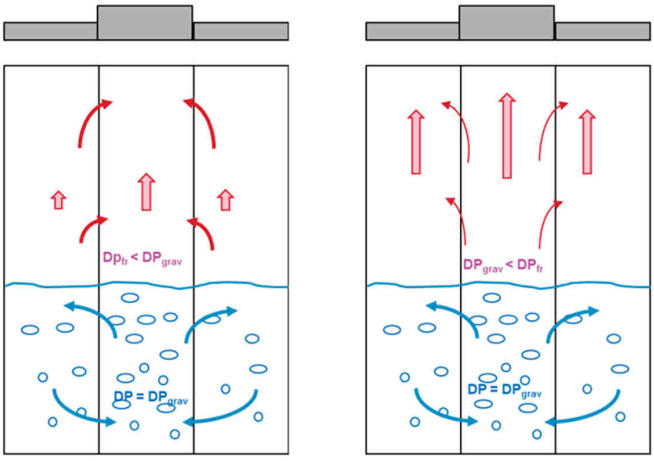

Fig. 1: Chimney (left) and diverging (right) effect phenomena (radial power profiles appear in grey).

2.2. Crossflows Direction Identification

In a single-phase flow situation in a steady situation (like the dry zone), momentum equation is (turbulent and dispersive effects can be neglecting in this analyze [10]):

$$\rho\left(\vec{V}\nabla.\vec{V}\right) + \nabla P = \rho\vec{g} + \tau_w \tag{1}$$

First, we suppose that there is no radial cross-flow in the dry zone of the core. Thus, we will demonstrate that when there is a radial power profile in the core, the axial pressure evolution along the dry zone is not the same between assemblies. Cross-flows between assemblies are then necessary to equalize pressure.
If only axial flow is considered in the dry zone, momentum equation in the axial direction can be written:

$$\rho\left(V_z\frac{\partial V_z}{\partial z}\right) + \frac{\partial P}{\partial z} = -\rho g - \frac{K_{eff_Z}}{D_{H_z}}\rho\frac{{V_z}^2}{2} \tag{2}$$

With: $K_{eff_Z} = \frac{D_{H_z}K_{SG_Z}}{\Delta z_{SG}} + C_{f_Z}$ the axial friction loss coefficient (for rods and mixing grids). The following calculations will use Blasius law for C_{f_Z} ($C_{f_Z} = 0.316\,Re^{-0.25}$) ; $K_{SG_Z} = 1$ (head loss coefficient for one mixing grid) and $\Delta z_{SG} = 0.52\ m$ (the distance between two mixing grids). D_{H_z} is the hydraulic diameter and is taken equal to 0.011 m ($D_{H_z} = \frac{4\,S}{\chi}$).
The axial acceleration can be evaluate with the local heat flux (for a constant mass flux - G_v):

$$\frac{\partial V_z}{\partial z} = G_v\frac{\partial\left(\frac{1}{\rho}\right)}{\partial z} = \frac{-G_v}{\rho^2}\frac{\partial\rho}{\partial z} = -\frac{V_z}{\rho}\frac{\partial\rho}{\partial z} = -\frac{V_z}{\rho}\frac{\partial\rho}{\partial T}\frac{\partial T}{\partial z} = \alpha\,V_z\frac{\partial T}{\partial z} \approx \alpha\,V_z\frac{4\,\Phi_{loc}}{G_v\,C_{pv}\,D_{H_z}} \tag{3}$$

With $\alpha = -\frac{1}{\rho}\frac{\partial\rho}{\partial T}$ the vapor isobaric dilatation coefficient (K^{-1}); Φ_{loc} the local wall heat flux (W/m^2); G_v the vapor mass flux ($kg/s/m^2$) and C_{pv} the vapor specific heat capacity (J/kg/K).
With (2) and (3), the axial evolution of the pressure gradients is:

$$\frac{\partial P}{\partial z} \approx -\rho g - \rho{V_z}^2\left(\frac{K_{eff_Z}}{2\,D_{H_z}} + \frac{4\,\alpha\ \Phi_{loc}}{G_v\,C_{pv}\,D_{H_z}}\right) \tag{4}$$

The equation (4) is derivate with respect to the density for a constant vapor mass flux (G_v):

$$\left(\frac{\partial\frac{\partial P}{\partial z}}{\partial\rho}\right)_{G_v} \approx -g + {V_z}^2\left(\frac{K_{eff_Z}}{2\,D_{H_z}} + \frac{4\,\alpha\ \Phi_{loc}}{G_v\,C_{pv}\,D_{H_z}}\right) \tag{5}$$

Thank to: $\left(\frac{\partial(\rho{V_z}^2)}{\partial\rho}\right)_{G_v} = \left(\frac{\partial\left(\frac{{G_v}^2}{\rho}\right)}{\partial\rho}\right)_{G_v} = -\frac{{G_v}^2}{\rho^2} = -{V_z}^2$ and $C_{f_Z}\sim(\rho V_z)^{-0.25}\sim{G_v}^{-0.25}$ ➔ $\left(\frac{\partial K_{eff_Z}}{\partial\rho}\right)_{G_v} = 0$

We assume neglecting vapor properties (α, μ, C_{pv}) variations with ρ variation.
Considering V_0, the axial gas velocity at the swell level, we define F_1 number:

$$F_1 = \frac{{V_0}^2\left(K_{eff_Z} + \frac{8\,\alpha\ \Phi_{loc}}{G_v\,C_{pv}}\right)}{2g\,D_{H_z}} \tag{6}$$

Assuming that liquid phase under the swell level is at the saturation temperature, V_0 (and G_v) can be evaluated with:

$$V_0 = \frac{4\int_0^{H_{swell}}\Phi(z)dz}{\rho_{sat}\,\Delta H_{l\to v}\,D_{H_z}} \tag{7}$$

With H_{swell}, the swell level (m); ρ_{sat}, the vapor density at saturation (kg/m^3); $\Delta H_{l\to v}$, the latent heat of vaporization (J/kg) and $\Phi(z)$, the wall heat flux (W/m^2).

Expression (5) sign depends on F_1 value: $F_1 < 1 \Rightarrow \left(\frac{\partial \frac{\partial P}{\partial z}}{\partial \rho}\right)_{G_v} < 0$; $F_1 > 1 \Rightarrow \left(\frac{\partial \frac{\partial P}{\partial z}}{\partial \rho}\right)_{G_v} > 0$

As ρ variations are the most important in the highest power assembly (due to the heating), $\frac{\partial P}{\partial z}$ variations are most important too. Because of the swell level is almost uniform, the pressure is radially homogeneous just above it. Moreover, one can see that $\frac{\partial P}{\partial z}$ is always negative (equation 4) in the dry zone. Thus, in the dry zone, to compensate different pressure gradients between assemblies, cross-flows must take place between highest power assembly and others. The cross-flow direction depends on F_1 value:

- $F_1 < 1 \Rightarrow \left(\frac{\partial \frac{\partial P}{\partial z}}{\partial \rho}\right)_{G_v} < 0 \Rightarrow 0 > \frac{\partial P}{\partial z}\Big)_{low\ power\ assemblies} > \frac{\partial P}{\partial z}\Big)_{high\ power\ assembly}$

  The pressure loss is more important in the highest power assembly than in the others, pressure is thus lower in the highest power assembly.

  ➔ **Cross-flows are going from the low power assemblies to the higher power ones.**

- $F_1 > 1 \Rightarrow \left(\frac{\partial \frac{\partial P}{\partial z}}{\partial \rho}\right)_{G_v} > 0 \Rightarrow \frac{\partial P}{\partial z}\Big)_{low\ power\ assemblies} < \frac{\partial P}{\partial z}\Big)_{high\ power\ assembly} < 0$

  The pressure loss is less important in the highest power assembly than in the others, pressure is thus higher in the highest power assembly.

  ➔ **Cross-flows are going from the higher power assemblies to the low power assemblies.**

To conclude, evaluating F_1 value just above the swell level gives an indication of the cross-flows direction in the dry zone.

$$F_1 < 1 \ \ Chimney\ effect\ ;\ F_1 > 1\ Diverging\ effect$$

2.3. Main Parameter Influencing Cross-Flows Phenomenology in the Dry Zone

From the expression of F_1 (equation 6) and V_0 (equation 7), one can see that the main parameters influencing cross-flows phenomenology in the dry zone are:

- The pressure (mainly through ρ_{sat} variations)
- The power decay heat flux
- The swell level elevation

Fig. 2 gives an overview of the F_1 number sensibility to these parameters. One can see, at left, the swell level elevation influence, and at right, the pressure influence. Decay power heat flux level influence is visible on both curves. All F_1 numbers are calculated with a nominal power (NP) of 61.3kW/cm² and axial power profile is a cosine. For the pressure influence, calculation have been made with a swell level elevation at 2.5m (the core is 3.66 m high).

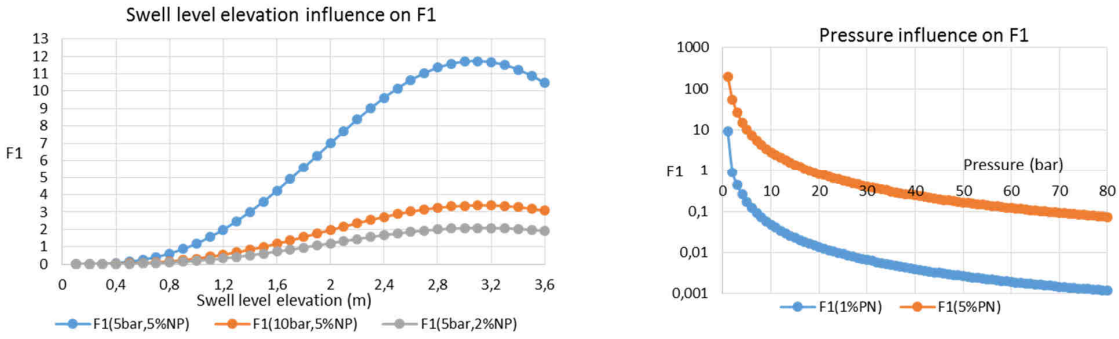

Fig. 2: The swell level elevation influence (left) and the pressure influence (right) on F_1

From the Fig. 2, the following tendencies can be written:

- "Chimney" effect could be observed at high pressure when "Diverging" effect can only occurs at low pressure,
- Low power decay heat flux favors "Chimney" effect,
- "Chimney" effect can occur at low pressure and high power decay heat flux when the swell level is low,
- The axial power profile have also an influence on F_1 number, when the swell level reach the top of the core, F_1 decrease due to Φ_{loc} contribution which reach 0.

2.4. "Chimney" and "Diverging" Effect at Sub-channel Scale

In the dry zone, at sub-channel scale, radial densities gradients are higher at the boundary region between the highest power assembly and the others. Thus, cross-flows occurring during "Chimney" and "Diverging" effects mainly impacts the boundary layers between assemblies. Specific behaviors may then be spotted at sub-channel scale:

- In case of "Chimney" effect: cross-flow are going from the low power assemblies to the high power one. External regions of the high power assembly receive more steam than the central region. The PCT may thus occurs at the center of the high power assembly. Moreover, the vapor received by the high power assembly from the others is cooler that increase the benefits of "Chimney" effect on PCT.
- In case of "Diverging" effect: cross-flow are going from the high power assembly to the others. External regions of the high power assembly receive less steam than the central region. PCT may thus occur at the periphery of the high power assembly.

Fig. 3 presents both cases.

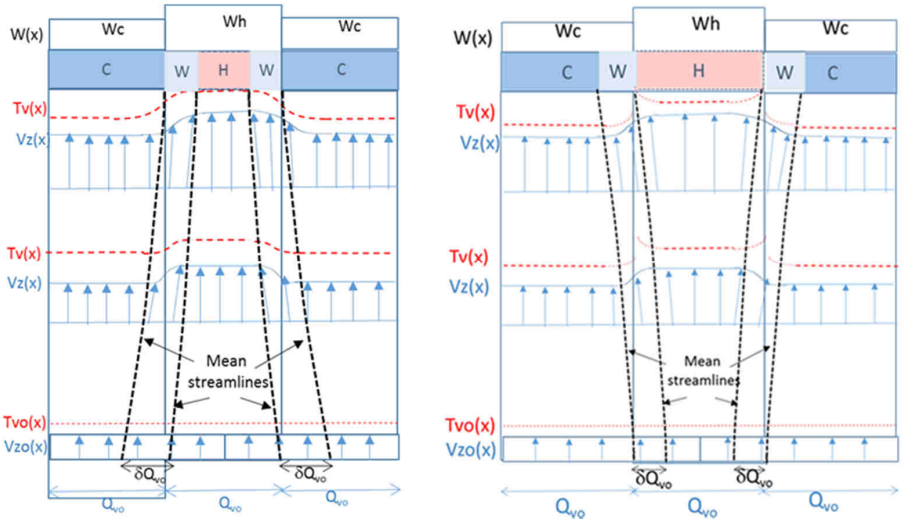

Fig. 3: Chimney (left) and diverging (right) effects phenomena at sub-channel scale in the dry zone

3. EXPERIMENTAL EVIDENCES OF DIVERGING AND CHIMNEY EFFECTS

In this part, experimental evidences of diverging and chimney effects during core uncovering phases will be shown. First, "Diverging" effect will be observed on low pressure experimental tests: PERICLES-2D BOIL-UP. Then, "Chimney" effect is spotted on high pressure core uncovering phases during test 3 of ROSA-2 Project.

3.1. Diverging Effect Evidences

The PERICLES 2D experimental program was partly embedded in the Shared Cost Action Program (SCA) of the European Communities (CEC) on Reactor Safety, Research Area No. 4, concerning the analysis of experimental data on LOCA and emergency core cooling [12]. Experimental facility is first described, before analyzing experimental data that lead to diverging effect observation.
The PERICLES 2D experiment had been carried out to investigate multidimensional effects which can occur in a PWR core where heating power is not radially uniform during core uncovering phase (relative to SBLOCAs) and also reflooding phase (relative to LBLOCAs). The experiment consists of a vertical rectangular section containing three different rod assemblies, denoted here by A, B and C. Each assembly contains 7* 17 = 119 full length heater rods. The dimensions of the assemblies are indicated in Fig. 4 – left.

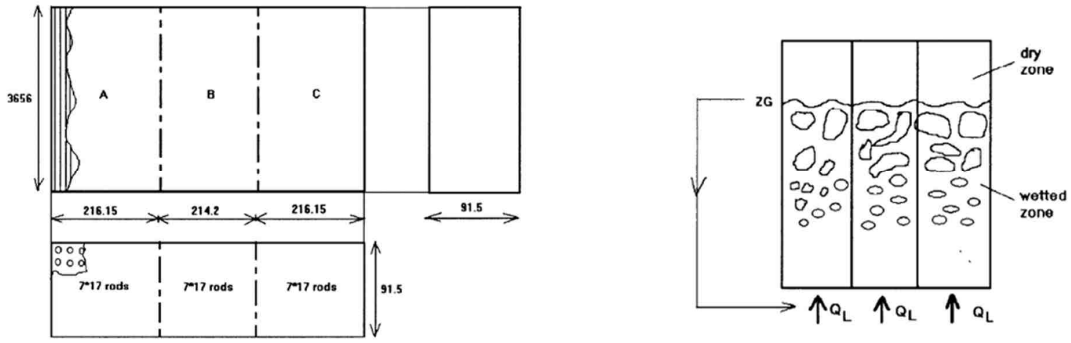

Fig. 4: The PERICLES 2D experiment (dimensions in mm) – left – and the BOIL-UP tests – right

The assemblies are heated by two independent electrical power sources, giving the possibility of increasing more the central assembly B power ('hot' assembly) than the two lateral ones A and C ('cold' assemblies). The heated length of the rods is 3656 mm and the rod diameter is equal to 9.5 mm.
Rods power is not uniform, but depends on the axial position (elevation). All rods have the same axial heating profile, with higher flux density at mid-length. The nominal heat flux densities ϕ in the lateral assemblies A and C are identical which allow us to define $\phi(B)/\phi(A,C)$ as the radial peaking ratio. In the different tests investigated, the nominal values of the heat flux densities ranged from 2.45 W/cm² to 5 W/cm², with given values of the radial peaking factor F_{XY} between 1 and 1.85. Pressure at the exit of the section was equal to 3 bar. The cladding temperature is measured by means of thermocouples; in each assembly, the cladding temperature is measured at 24 different elevations.
In the BOIL-UP tests of the PERICLES 2D experiment, some subcooled water (60 °C under saturation temperature) enters into the section at the bottom. Rods are electrically heated and some vaporization occurs along the channel. Flow is successively a single-phase liquid then two-phase mixture and finally single-phase vapor flow. The transition between the two-phase zone and the dry zone (single-phase vapor) occurs at the elevation of the swell level ZG (Fig. 4 – right).
The liquid flow rate (Q_L) at the injection is regulated in order to have a given stationary elevation of the swell level. The controlling parameters were the nominal values of the wall to fluid heat flux densities in the three assemblies and the inlet liquid flow rate corresponding to a stationary elevation of the swell level ZG (Fig. 1– right). The swell level elevations in the different tests ranged from 2.20 m to 3.45 m and were approximately the same for the three assemblies, even if radial peaking factor is not equal to 1.
In order to simulate LOCA transient CATHARE code has been validated against these tests using a coarse radial meshing of one mesh per assembly [13]. Following discussions will next focus on three tests with the same swell level elevation (2.74m), with different radial peaking factors F_{XY}: 1, 1.43 and 1.85. In order to analyze measurements of the cladding temperature in the dry zone of the hot assembly (B). Fig. 5 presents its horizontal section and the localization of the thermocouples at two elevations (3.2m and 3.4m). The thermocouples next to the lateral walls were not taken into account.

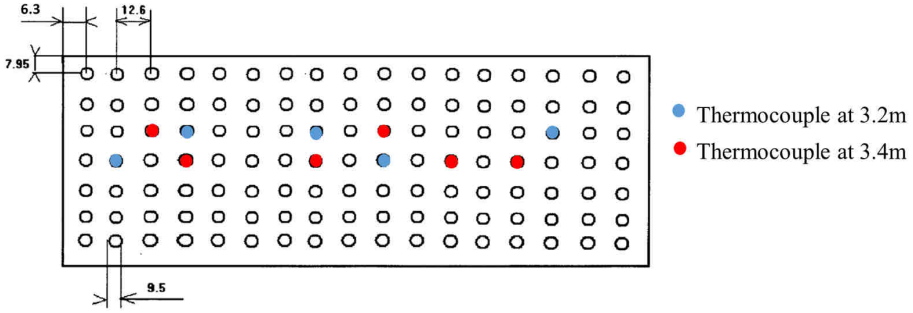

Fig. 5: Horizontal section of the hot assembly with the thermocouple positions (dimensions in mm)

Cladding temperature differences (between the maximum and the minimum temperature for each test) in the central assembly are shown in Fig. 6 for two elevations in the dry zone: 3.2m and 3.4m.

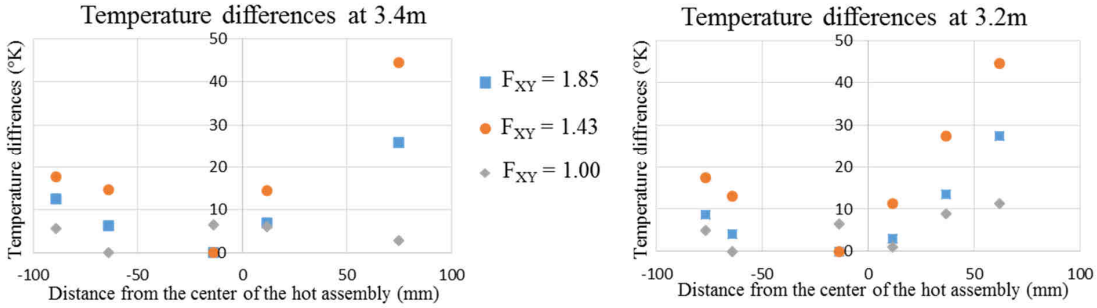

Fig. 6: Cladding temperature differences in the hot assembly of the PERICLES-2D Boil-Up tests for two elevations of the dry zone

For a radial peaking factor of 1 (grey dots on Fig. 6), the differences are not relevant, with a maximum of 10°K which is explain by the fact that no cross-flow are expected due to equal power in the 3 assemblies. It shows that the experimental data dispersal is low enough to draw conclusion for the other tests.
Magnitude of the F_1 number for the tests with higher peaking factors could be evaluated this way (assuming all the water vaporize in the wetted zone):

- the order of magnitude of the inlet flowrate (Q_L) is 0.5kg/s,
- S is the test section,

$V_0 = \frac{Q_L}{S * \rho_{sat}} \cong 8.9\ m/s$

Which lead us to (according that local heat flux at the swell level is about 5W/cm² in the hot assembly)
$F_1 \cong 30$
"Diverging" effect is then clearly expected is these tests, with cross-flows going from the hot assembly to the cold as detailed in part 2. Moreover, these cross-flows should create boundary mixing layers and provide a maximum temperature (for both vapor and cladding) in the periphery region of the hot assembly (see Fig. 3 - right). This phenomena is observed on cladding temperatures plotted on Fig. 6 for both elevations. Moreover, total power injected in the test section is about 15% higher in the test F_{XY}=1.43 than in the test F_{XY}=1.85. This also leads to a value of V_0 about 15% higher and then a value for F_1 number about 32% higher. This can explain why temperature differences are more important in the test F_{XY}=1.43 than in the test F_{XY}=1.85. Analysis we have made of the results provided by the BOIL-UP tests of the PERICLES 2D experiment tends to constitute a clear evidence of the "Diverging" effect occurrence.

3.2. Chimney Effect Evidences

The OECD/NEA ROSA-2 Project [14] was performed to solve key safety issues of PWR Thermal-hydraulics by means of LSTF experiments conducted thanks to the Japan Atomic Energy Agency (JAEA). The core component of the experimental facility is first described as the Test 3, then, experimental data are analyzed, and point out a chimney effect occurrence.

LSTF is a full-pressure and full-height integral test facility using a full-height core composed of 1008 simulated fuel rods with 10 MW electrical power of 3.66 m heating length. Rods are gathered in 24 assemblies with a radial power profile split in 3 zones (high, mean and low). The radial peaking factor is 1.5 for the high power assemblies, 1.0 for the mean power assemblies and 0.66 for the low power ones. Fig. 7 gives an overview of the radial power distribution. All electrical fuel rods have the same cosine-shaped axial power profile. Test 3 is a Hot-Leg SB-LOCA transient during which core uncovering phases takes place two times:

- The High Pressure phase that longs for about 250s at around 7MPa, during which, the maximum measured cladding temperature was 780K [14].
- The Mean Pressure phase that longs for about 400s at around 4MPa, during which, the maximum measured cladding temperature was 822K [14].

For both cases, liquid level drop down to half the height of the core by boiling-of and core temperature excursion occurs in the dry zone. Experimental data package provide heating rods cladding temperatures (localized at the center of the assemblies) and gas temperatures (localized at the corner of the assemblies on non-heated rods) for several elevations in the dry zone. We will focus only on a quarter of the core, thanks to the symmetrical radial power distribution. We thus manage to regroup all temperatures measurements in the same quarter considering the core behavior is symmetrical. Fig. 7 presents the thermocouples localization (TW for the wall cladding temperature and TE for the fluid temperature) in a quarter of LSTF core at two different elevations in the dry zone.

At elevation 7, TW287, TW341 for clad and TE283, TE277 for fluid thermocouples come from different quarters of LSTF core and are localized on the same radial corner thanks to symmetrical considerations (same process is applied for TE293 and TE226 thermocouples at elevation 8). This test has been used to validate the 3D module of CATHARE at the assembly scale [15].

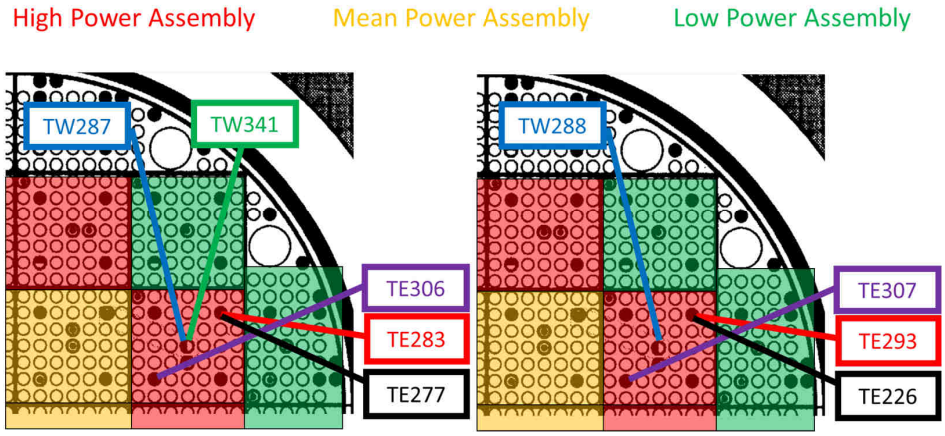

Fig. 7: Thermocouple localization in the high power assembly for elevation 7 (left) and 8 (right) of the LSTF core – High Power Assemblies are in red, Mean Power ones in yellow and Low Power ones in green

Let's compute an order of magnitude of the F_1 number for the two core uncovering phases. The total power (P_W) in the LSTF core is about 1.4MW for the High Pressure phase and 1.2MW for the Mean Pressure phase, which lead us to (with S is the core section and we assume that swell level is at core mid height) :
$V_0 = \frac{P_W * 0.5}{S\,\rho_{sat}\,\Delta H_{l\to v}} \cong 0.11\ m/s$ for the high pressure phase and $V_0 \cong 0.15\ m/s$ for the mean pressure phase.
At mid height, the axial power peak factor is equal to 1.5, which led us to a F_1 number of 0.006 for the high pressure phase and 0.012 for the mean pressure phase. "Chimney" effect is thus clearly expected in these cases with cross-flows coming from the low power assemblies to the high power ones.
Fig. 8 and Fig. 9 show the experimental temperature evolutions for elevation 7 and 8 during both phases.

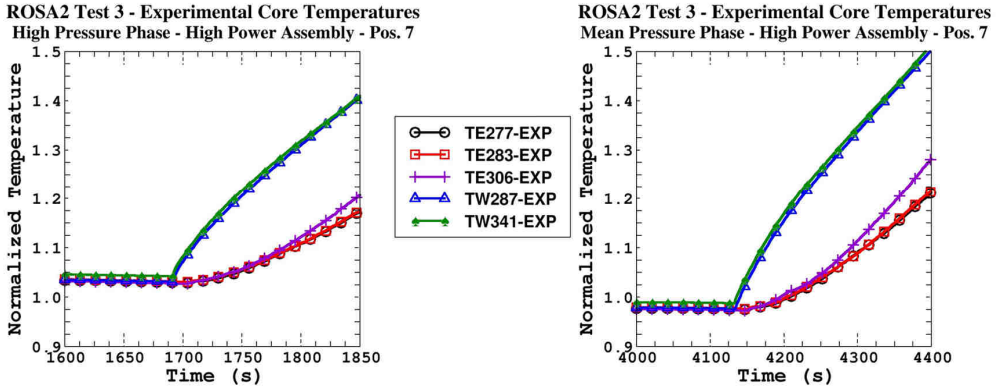

Fig. 8: Temperature evolutions at elevation 7 for the High (left) and Mean (right) Pressure phases

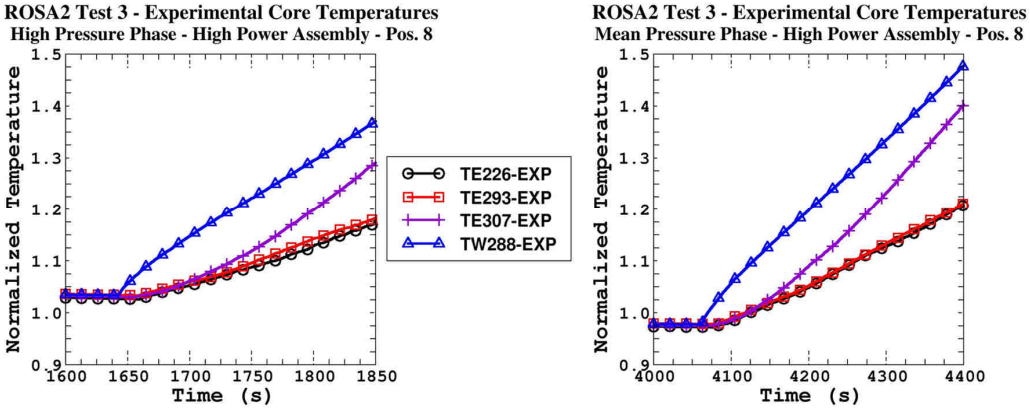

Fig. 9: Temperature evolutions at elevation 8 for the High (left) and Mean (right) Pressure phases

First, one can see that TE277 and TE283 evolutions on Fig. 8 as TW287 and TW341 evolutions on Fig. 8 and TE226 and TE293 evolutions on Fig. 9 are similar which confirm the symmetrical behavior of the core during the core uncovering phases.
Moreover, all fluid temperature thermocouples are localized at a corner of the high power assembly, one row away from the assembly boundary. If cross-flow between assemblies does not exist, their evolutions should be the same.
TE306 at elevation 7 and TE307 at elevation 8 are localized next to one high power assembly and one mean power assembly while the other fluid temperature thermocouples (TE283, TE277 at elevation 7 and TE293, TE226 at elevation 8) are localized next to two low power assemblies. As ρ gradients between assemblies are more important at the boundary of high/low power assemblies than at the boundary of high/mean and high/high power assemblies, "Chimney" effect is also expected to be more important between high/low

power assemblies. It should bring some 'cold' steam from the low power assemblies to the high power one. This phenomena is clearly observed for both phases and both elevations on the experimental evolutions with a steam temperature lower next to the low power assemblies (TE293 vs TE307 at elevation 7 and TE283 vs TE306 at elevation 8). Steam temperature differences exhibits a value higher than 50°C. It finally appears that analysis of data provided by LSTF facility constitute a direct evidence of the "Chimney" effect on the experimental Test 3.

3.3. Conclusion on Experimental Evidences

In this part, experimental evidence of "Chimney" and "Diverging" effects have been shown. They confirm that 3D effect are present during LOCA in the dry zone of the core and that analysis made in part 2 is reliable. The impact of cross-flows on cladding temperature are not negligible: 40°C for PERICLES-2D BOIL-UP test and more than 50°C on vapor temperature in ROSA2 test 3 core uncovering phases. For system codes' 3D modules it is then a safety issue to provide an accurate modelization of these phenomena. CATHARE simulations at sub-channel scale of PERICLES-2D BOIL-UP test [11] and ROSA2 test 3 core uncovering phases [16] have been made and they show that two points have an impact on the boundary mixing layer between assemblies:

- The transversal wall friction modelling
- The turbulent and dispersive models

Unfortunately, the experimental data on PERICLES-2D and LSTF are not sufficient to calibrate and validate these models. Nevertheless, calculations [11] [16] show that CATHARE is able to reproduce the right tendencies at sub-channel scale.
The experimental program METERO [11], which will be made at CEA, will provide more information which are necessary for the development and the validation of turbulent diffusion and dispersion terms as for transversal head loss in rob bundle geometry. METERO test section is composed by two half PWR assemblies and has the objective to enhance the validation of the models involved in 3D simulations of the core behavior during PWR LOCA.

4. CATHARE SIMULATIONS OF CHIMNEY EFFECT

CATHARE simplified simulations of the dry zone (only two assemblies modeled) have already been presented [10], they show that the expected cross-flow are well computed. In this part, a more complex simulation (close to a real PWR core) is detailed, showing "Chimney" effect and its impacts on the PCT.

4.1. Main assumptions

Actual nodalizations used with CATHARE for core behavior analysis, during a LOCA transient, is composed by a 2D cylindrical mesh divided in three main crowns of various power (Fig. 10 at left). As explained in part 2, cross flows are mainly due to the radial power difference between the crowns when core is uncovered. In order to investigate the crossflow that could occur in these specific reactor conditions, the modelisation had been simplified by cropping the core in the radial direction. Thus, a new cartesian mesh had been built in order to represent 8 assemblies of the core radius (Fig. 10 at right). It has to be mentioned that this modelisation uses the same geometrical parameters (hydraulic diameters, pressure loss coefficient, porosities) and power discretization (radial and axial profiles) as the complete reactor one. The axial power is cosine distributed and it is decreasing from right to left (power factors: 1.6 in C1, 0.99 in C2 and 0.94 in C3). In order to represent thermohydraulic conditions of the PCT occurrence, a stabilized swell level is first obtained by the injection in the lower plenum (under the 3D element) of the reactor flowrate associated to the core uncovering. It correspond to the LOCA transient instant when system pressure is almost 45 bar. End of calculation, which had been run during thousands seconds to ensure results convergence, leads to a stabilized state with a radially homogeneous swell level. Void fraction obtained at this moment in the assemblies is shown on Fig 11.

4.2. Liquid phase behavior under swell level

Before looking at the cross flow occurrence in the gas phase, a short analysis of liquid behavior under the swell level showed that it behaves the same as during the whole LOCA reactor transient calculation. Indeed, because of the higher power of the left assemblies, and the lower of right ones, liquid tends to flow down at right to the lower plenum volume before being reinjected in the hot assemblies at left and starting its vaporization. Thus, it has to be noticed that the convection structure created between hot and cold assemblies crosses the lower plenum the same as for reactor simulations.

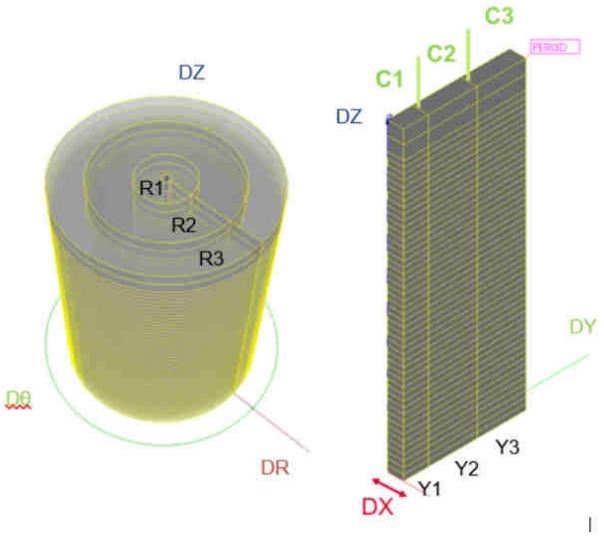

Fig. 10: 3D representations of a PWR core –Left– sensibility studies –Right–

Fig. 11 shows also that, as mentioned in part 2.2, the swell level is almost uniform at 1.9 m and the pressure is radially uniform for the gas phase at this elevation.

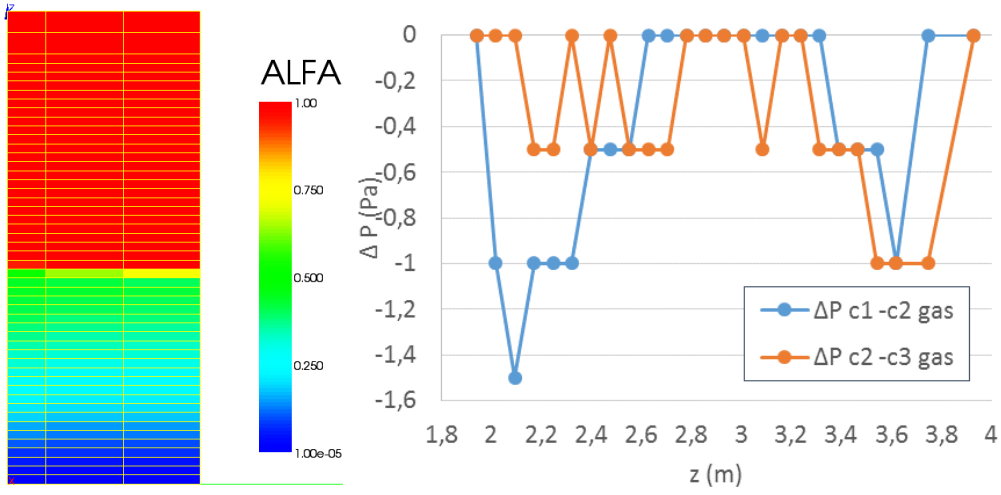

Fig. 11: Void fraction distribution at the end of calculation –Left– Pressure differential between columns –Right–

4.3. Gas phase behavior above swell level

In the simulated case, the fuel rod hot spot (where PCT takes place) is located at around 3.5 m height. At this point, cooling is only ensured by steam flow which characteristics depend on "chimney" or "diverging" effect. An evaluation of F_1 number above the swell level have thus been made. The order of magnitude of the inlet flowrate (Q_L) is 1.1kg/s which gives (assuming all the water vaporize in the wetted zone; S is the test section):$V_0 = \frac{Q_L}{S* \rho_{sat}} \cong 0.26\ m/s$. It leads to (the local heat flux at the swell level is about 2.5W/cm² in the hot assembly) the value $F_1 \cong 0.04$. It could thus be observed on Fig. 12 (Left part), very quickly above the swell level, that cross flows from C2 to C1 and from C3 to C2, representative of the chimney effect, take place. They could mainly be attributed to the difference of steam densities between the columns (see right part on Fig. 12). Nevertheless, if chimney effect remains from the swell level to the top of the core, its intensity decrease as we come closer to the hot spot. This effect is mainly due to cross flows which tend to equilibrate density gap between columns.

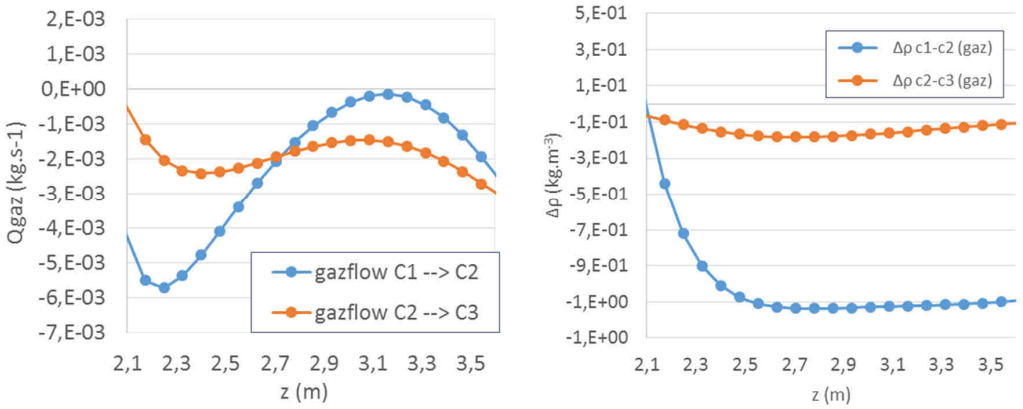

Fig. 12: Cross flows between columns –Left– Density differential between columns –Right–

These observations are confirmed by plotting the mass flux (see Fig. 13.): although for columns 2 and 3 mass flux keeps in between 5 and 6 kg.m^{-2}.s^{-1}, it increases briefly to 7.5 kg.m^{-2}.s^{-1} for column 1 between 1,98 m and 2.74 m.

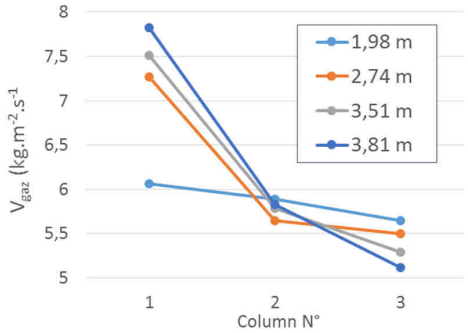

Fig. 13: Mass flux at various height for the 3 columns

Results provided by the simulation presented in this part, based on the modelisation in use for PWR LOCA transient analysis, confirm that chimney effect occurs during core uncovering. Nevertheless it has to be mentioned that cross flows, providing coolant to the hot assemblies in this case, are mainly observed just above the swell level and tend to decrease when flow goes up in the core. An equilibrium situation is thus

obtain up in the core when axial density variations are almost the same in all assembly. As shown in Fig. 12, cross-flows decrease when $\Delta\rho$ between assemblies is almost constant with the elevation.

4.4. Transversal head losses sensibilities

In order to evaluate the influence of cross flow cooling on the PCT, transversal head loss have been artificially modified by using a multiplying coefficient on the lateral faces of the mesh. It have to be specified that transversal head loss coefficient have only been applied above the swell level in order not to modify liquid phase behavior. Head loss coefficients used and PCT obtained next are summarized in the following table. As expected it, could be observed that transversal head losses have a direct influence on cross flow between the assemblies according to the variation of PCT. An increase of transversal head losses leads to a chimney effect reduction that consequently limit the amount of hot spot cooling gas that comes from cold assemblies. PCT in regard is thus superior when head losses are increased.

Head loss	/10	ref	x10	x100
PCT (°C)	837	847	856	890

5. CONCLUSIONS

It was found that for PWR safety issues like LOCA accident, studies of physical phenomena that occur during uncovering phase of the core is of importance. During such situations a swell level tends to separate core in two parts: one with a mixture of gas and liquid at the bottom and one with pure steam at the top. According to the heterogeneous distribution of power between the assemblies in the core, acceleration of steam and density decrease, along the axial direction, could be different for high or low power regions. This unbalance introduce pressure difference and conduct to the existence of cross flow between assemblies.
In order to characterize these cross-flows, F_1 number, introduced previously by Bestion, is taken back on the bases of momentum equation for the steam phase. The final form obtained is:

$$F_1 = \frac{{V_0}^2\left(K_{eff_Z}+\frac{8\,\alpha\,\Phi_{loc}}{G_v\,C_{pv}}\right)}{2g\,D_{H_Z}} \text{ with } F_1 < 1\ Chimney\ effect\ ;\ F_1 > 1\ Diverging\ effect$$

It gives an indication of the cross flow direction above the swell level and appears also sensitive to pressure, level elevation and heat flux, that is to say power decay. “Chimney” effect could occur either at high or low pressure whether “Diverging” effect appears only at low pressure. Indeed low power decay heat flux tends to favors “Chimney” effect. At last it have been shown that the radial place of the hot spot in the hot assembly could change from center to periphery according to the type of cross flow established: chimney or diverging.
By this theoretical considerations, analysis of data provided by PERICLES 2D BOIL-UP test facility gave us an evidence of the occurrence of diverging effect between two low power peripheral assemblies and a higher power central one for low pressure. On another hand, Test 3 conducted on LSTF ROSA facility, with higher pressure, have also been analyzed and conduct to the observation of chimney effect according to the analysis of thermocouple temperature located near the interface of high/low power and high/medium power assemblies.
At last a simulation of a core slice, with boundary conditions extracted from whole reactor LOCA transient have been realized with CATHARE code. Results we obtained give an accurate representation of the exchange between assemblies of various power. Indeed, liquid phase under swell level behave in a convective way and pure steam phase above exhibit cross flows representatives of a chimney effect which is in good agreement with F_1 number evaluation for this case. Nevertheless, it has been observed that chimney effect is not constant all along the assemblies and highly depends on transversal head loss. In this way it can be expected that METERO experimental program, which will be carry on at CEA, will provide more information to enhance our understanding and to model with accuracy “Chimney” or “Diverging” effects that should also been taken into account for Core Exit Temperature (CET) analyses [17].

ACKNOWLEDGMENTS

CATHARE code is developed in the framework of the NEPTUNE project, supported by CEA, EDF, FRAMATOME and IRSN. This work has been financially supported by CEA, EDF, and FRAMATOME.

REFERENCES

1. O. Antoni and all, "CATHARE 2 V2.5_2: a single version for multi-applications", *Nuclear Engineering and Design*, **241**(11), pp. 4456-4463 (2011)
2. J. Dufrêche and I. Dor, "Assessment of the CATHARE 3D module with UPTF downcomer refill tests" *Proceedings of 40th European Two-Phase Flow Group Meeting*, Norway, 2003
3. I. Dor and P. Germain, "Core radial profile effect during reflooding, validation of CATHARE 2 3D module using SCTF tests", *NURETH-14*, Toronto, Canada, Sept. 25-30, 2011
4. I. Dor, C. Morel, P. Bazin and P. Boudier, "Assessment of the CATHARE 3D module for LBLOCA simulation", *NURETH-11*, Avignon, France, Oct. 2-6, 2005
5. R. Prea, V. Figerou, A. Mekkas and A. Ruby, "CATHARE-3: a first computation of a 3-inch break loss-of-coolant accident using both Cartesian and cylindrical 3D meshes modelling of a PWR vessel", *NURETH-17*, Xi'an, China, Sept. 3-8, 2017
6. H. Geiser, J.L. Vacher, and P.R. Rubiolo, "The use of integral effects tests for the justification of new evaluation models based on the BEPU approach", *NURETH-17*, Xi'an, China, Sept. 3-8, 2017
7. D. Pialla, M. Ludmann, K. Vareille, "Preliminary tasks to integrate CATHARE 3D reactor pressure vessel module in real-time simulators at EDF/DT", *NURETH-18*, Portland, OR, USA, Aug. 18-22, 2019
8. C. Herer and all, "3DSYSTH : an OECD/NEA activity on multi-dimensional capabilities of thermalhydraulics system", *ICAPP'19*, Juan les Pins - French Riviera, May 12-15, 2019
9. D. Bestion and L. Matteo, "Scaling considerations about LWR core thermalhydraulics", *NURETH-16*, Chicago, IL, USA, Aug. 30-Sept. 4, 2015
10. D. Bestion, P. Fillion, P. Gaillard, M. Valette, "3D core thermalhydraulics phenomena in PWR SB-LOCAs and IB-LOCAs", *NURETH-17*, Xi'an, China, Sept 3-8, 2017
11. D. Bestion, P. Fillion, R. Préa, G. Bernard-Michel, "Improved PWR LOCA simulations through refined core 3D simulations – An advanced 3D modelling and the associated METERO validation program", *NUTHOS-12*, Qingdao, China, Oct. 14-18, 2018
12. R. Deruaz, P. Clement, J.M. Veteau, "2D effects in the core during the reflooding phase of a LOCA, Safety of Thermal Water Reactors", *Proceedings of a Seminar on the Results of the European Communities' Indirect Action Research Programme on Safety of Thermal Water Reactors*, Brussels, Belgium, Oct. 1-3, 1984, Published in 1985 by Graham & Trotman Limited
13. C. Morel and D. Bestion, "Validation of the CATHARE code against PERICLES 2D BOIL-UP Tests", *NURETH-9*, San Francisco, CA, USA, Oct. 3-8, 1999
14. OECD/NEA, "Final Integration Report of the Rig-of-Safety Assessment (ROSA-2) Project – 2009-2012", NEA/CSNI/R(2016)10
15. R. Préa, "Validation of CATHARE 3D module on LSTF Core", *NURETH-18*, Portland, OR, USA, Aug. 18-22, 2019
16. R. Préa and A. Mekkas, "Rod bundle thermalhydraulics mixing phenomena: 3D analysis with CATHARE-3 of ROSA-2/LSTF experiment", *Proceedings of the "Turbulence and Interaction" Conference (TI-2018)*, Les Trois Ilets, Martinique, France, June 25-29, 2018
17. OECD/NEA, "Core Exit Temperature (CET) Effectiveness in Accident Management of Nuclear Power Reactor", NEA/CSNI/R(2010)9